The Potential Vorticity Structure of Equatorial Deep Jets

JOANNA MUENCH AND ERIC KUNZE

School of Oceanography, University of Washington, Seattle, Washington

ERIC FIRING

Joint Institute for Marine and Atmospheric Research, University of Hawaii, Honolulu, Hawaii

ABSTRACT

The equatorial deep jets are often modeled as equatorially trapped long waves, either Kelvin or Rossby. Rossby waves perturb potential vorticity but Kelvin waves do not; therefore the potential vorticity structure of a 16-month mean velocity section from 3°N to 3°S on 159°W is examined. To distinguish the equatorial deep jets from flow components with larger vertical scales, the mean profiles were decomposed into a low-vertical-mode component and a residual, dominated by the deep jets. The deep jets resemble a first-meridional-mode Rossby wave; their velocity at 2°N and 2°S is opposite in direction to their velocity on the equator, and consequently they show a potential vorticity perturbation. The zero crossings of the jets' zonal velocity are at 1°30'N and S, farther from the equator than the 1°N and S predicted by linear wave theory. One possible explanation for this broadening is meridional advection of the jets by higher-frequency motions such as Rossby–gravity waves.

1. Introduction

Over the past two decades, observations have revealed a series of deep zonal currents below the equatorial undercurrent in the Pacific, Indian, and Atlantic oceans. Luyten and Swallow (1976) first observed the deep jets on the equator in the Indian Ocean. During one month of observations, they found strong steady zonal velocities with small vertical scale extending below 3000 m. The jets were confined within two degrees of the equator. In the equatorial Pacific deep jets were found at many longitudes (Hayes and Milburn 1980; Leetmaa and Spain 1981; Eriksen 1981).

The Pacific Equatorial Ocean Dynamics (PEQUOD) experiment of 1981–1983 was designed to study these jets. The field study consisted of a moored current meter array maintained for two years (Eriksen 1985; Eriksen and Richman 1988), absolute velocity profiles taken during mooring deployment and recovery (Ponte and Luyten 1989), and a 16-month time series of velocity profiles, the Line Island Profiling Project (LIPP) (Firing 1987, 1988, 1989). The data collected during PEQUOD, combined with other studies, has begun to yield a composite picture of the deep jets. Their vertical and meridional structure is fairly well defined but their zonal and temporal variability is less clear.

Located on the equator, the jets are characterized by alternating east–west currents with instantaneous velocities up to 25 cm s^{-1}. They have vertical wavelengths of about 300 m, are found from 500- to 3000-m depth, and are confined within 2° of the equator (Firing 1987). Ponte and Luyten (1989) found the zonal velocities to be coherent over 10° of longitude. Two years, the longest period of observations, was insufficient to resolve the jets' temporal behavior (Eriksen 1985).

GEOSECS data from the Atlantic suggests the presence of strong deep currents on the equator there as well (Eriksen 1982). A single vertical profile at 0°, 32°W contains alternating jetlike structures (Ponte et al. 1990). However, further observations are necessary to determine whether these features have the same meridional structure, zonal coherence, and longevity as the jets observed in the Pacific.

Attempts have been made to interpret observations of the deep jets as linear equatorial waves. Analysis of data collected by Luyten and Swallow (1976) in the Indian Ocean revealed that a simple model of the jets as linear long Kelvin waves was inconsistent with the observed deep jets whose meridional widths of up to 2° are broader than the 1° predicted by linear wave theory (O'Neill and Luyten 1984). Eriksen (1982) hypothesized from phase relations between zonal velocity and displacement that the jets observed in the Pacific Ocean had the characteristics of Kelvin waves. Analysis of other velocity profiles from the central Pacific at
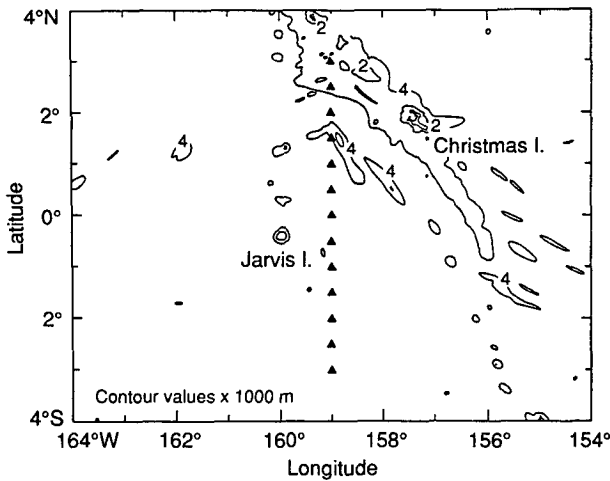
FIG. 1. Station locations and topography for the Line Islands Profiling Project (Firing 1987).

0°30'N and S, and 1°15'N and S showed reasonable agreement between the meridional scale of Kelvin waves and the observed deep jets, although the limited time span of the observations (15 months) prevented Ponte and Luyten (1989) from reaching any firm conclusion relating the deep jets to linear wave dynamics. Both their results and the results of Firing (1987) indicate that insufficient data exists to describe the temporal behavior of the jets.

Observations of the deep jets have been accompanied by many modeling attempts. Wunsch (1977) tried to model the deep jets observed in the Indian Ocean by Luyten and Swallow (1976) as linear long waves driven by monsoon winds, although subsequent analysis of the data (O'Neill and Luyten 1984) demonstrated contradictions between linear wave theory and the observed meridional scale of the deep features. McCreary (1984) found that time-dependent zonal wind forcing creates a complicated response of Kelvin and Rossby waves reflecting from the ocean surface, bottom, and lateral boundaries. His model produced jetlike structures, but the period of forcing, and therefore of the long waves, was at most one year, while observed deep jet time scales in the Pacific are much longer than two years. Subsequently, McCreary and Lukas (1986) hypothesized that stationary Kelvin waves, forced by a wind patch and Doppler shifted by a barotropic current, could produce deep zonal flows resembling the deep jets. The 15 cm s^{-1} westward current required in the model appears to be unrealistically large, however. McPhaden et al. (1986) proved that the propagation of high baroclinic mode Kelvin waves through strongly sheared flows, such as the equatorial undercurrent, is inefficient. Ponte (1989) modeled the deep jets as Kelvin and Rossby waves forced by a deep meridional boundary energy source.

If the deep jets are due to linear Kelvin or Rossby waves, they should share the characteristics of those waves. Specifically, the combined velocity and density structure should resemble that of a theoretical linear long equatorial wave. One of the distinguishing characteristics of these waves is their potential vorticity structure. Kelvin waves do not perturb potential vorticity, while Rossby waves do. Therefore, examination of the potential vorticity structure associated with the deep jets may indicate whether they can be modeled as either linear Kelvin or Rossby waves. This analysis is possible due to both the large number of sections available and the meridional resolution of the LIPP data.

2. Data and methods

Pegasus acoustic dropsonde profilers were used to obtain full water depth profiles of horizontal velocity and temperature in a section running from 3°N to 3°S at 159°W near the Line Islands (Fig. 1, Firing 1987). A total of 21 cruises were made from March 1982 to June 1983, resulting in 41 transects across the equator (Fig. 2). The profiles were smoothed in the vertical with a Gaussian filter (10-m standard deviation, 60-m total width, 76-m half-power wavelength) and subsampled every 20 m. [For a complete discussion of data collection and processing, see Firing (1987).]

The following analysis considers only the mean velocity structure from the 16-month time series. A time series of profiles (Fig. 3) establishes the persistence of the jets over the 16-month period of observation, with little discernible vertical motion. The standard error of the mean velocity components is 4 cm s^{-1} in the upper 500 m, and 1–3 cm s^{-1} at greater depths. The mean meridional velocity component is not statistically different from zero even though instantaneously it is as large as the zonal velocity; the meridional fluctua-
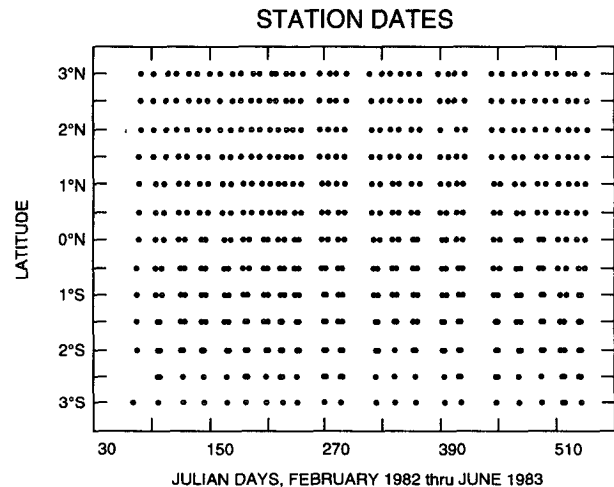

STATION DATES

FIG. 2. Profile latitudes as a function of time.
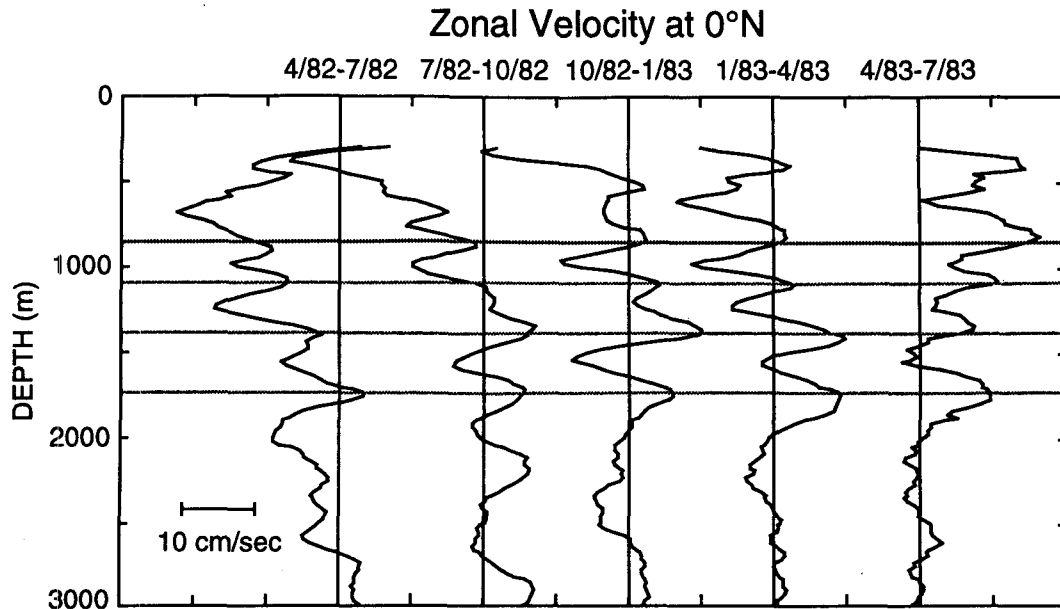
Zonal Velocity at 0°N

FIG. 3. Zonal velocity on the equator averaged over successive 3-month periods: (a) April 1982–July 1982, (b) July 1982–October 1982, (c) October 1982–January 1983, (d) January 1983–April 1983, (e) April 1983–July 1983. The gray lines are at 860 m, 1100 m, 1380 m, and 1740 m. The persistence of the jets is apparent over this 16-month period.

tions have much shorter time scales than the large zonal velocities.

In addition to the deep jets, Fig. 4 shows predominant extraequatorial currents with vertical scales of 500–1000 m, much larger than those of the deep jets. Assuming linearity, this unambiguous vertical scale separation suggests that the deep jets and the extraequatorial currents should be regarded as different phenomena and analyzed separately. Therefore, the mean zonal velocity field has been decomposed into a low-mode component and a high-mode residual, using linear vertical normal modes (Firing 1988). The vertical mean plus the first ten baroclinic modes are taken to be the low-mode component; mode 10 provides a natural separation point because its amplitude and standard deviation are both small. This choice of mode cutoff is also well separated from the mode range of the deep jets, which is around 33–36. The decomposition is used only as a method of scale separation.

The low-mode zonal velocity (Fig. 5a) includes the Equatorial Undercurrent, the South Equatorial Current, and several subthermocline currents discussed by Firing (1987, 1989). The residual zonal velocity (Fig. 5b) contains the deep jets and little else. Their vertical wavelength is 330 ± 70 m, and mean jet velocity is 4 ± 1 cm s^{-1}. Most of the jets are centered on the equator, although a few velocity extrema lie slightly off the equator at 30'N or S.

Potential vorticity was calculated separately for the low-mode and residual velocities. The Ertel potential vorticity is defined as

$$\Pi = (2\Omega + \nabla \times \mathbf{v}) \cdot \nabla b, \qquad (1)$$

where Ω is earth's rotation vector, $\mathbf{v}$ is the fluid velocity, and $b(y, z) = (g/\rho_0)[\bar{\rho}(z) - \rho(y, z)]$ is the buoyancy (overbar indicates average over latitude and time). Due to the observed geostrophic nature of the deep jets (Fig. 6), horizontal gradients in density may be expressed as

$$b_x \approx -\beta y v_z, \qquad (2a)$$

$$b_y \approx \beta y u_z. \qquad (2b)$$

Scaling allows simplification of the potential vorticity. (i) The horizontal gradients of vertical velocity are known to be small and may be neglected. (ii) The meridional velocity component and scale are small, so $v_x \ll u_y$. (iii) The horizontal component of earth's rotation vector is negligible in comparison to u_z.

Using the above approximations and assumptions, the potential vorticity used for this analysis is

$$q = \beta_y N^2 \quad -u_y N^2 \quad +\beta y b_z \quad -u_y b_z \quad -\beta_y (u_z)^2,$$
$$\text{planetary} \quad \text{relative} \quad \text{vortex-} \quad \text{nonlinear} \quad \text{twisting}$$
$$\text{vorticity} \quad \text{vorticity} \quad \text{stretching} \quad \text{vorticity/}$$
$$\text{stretching}$$

$$(3)$$

where

$$N^2 = g[(1/\rho)\bar{\rho}_z - g/C^2] \qquad (4)$$

is the buoyancy frequency (Millard et al. 1990).

The calculation of density from subthermocline Pegasus measurements is problematic because Pegasus
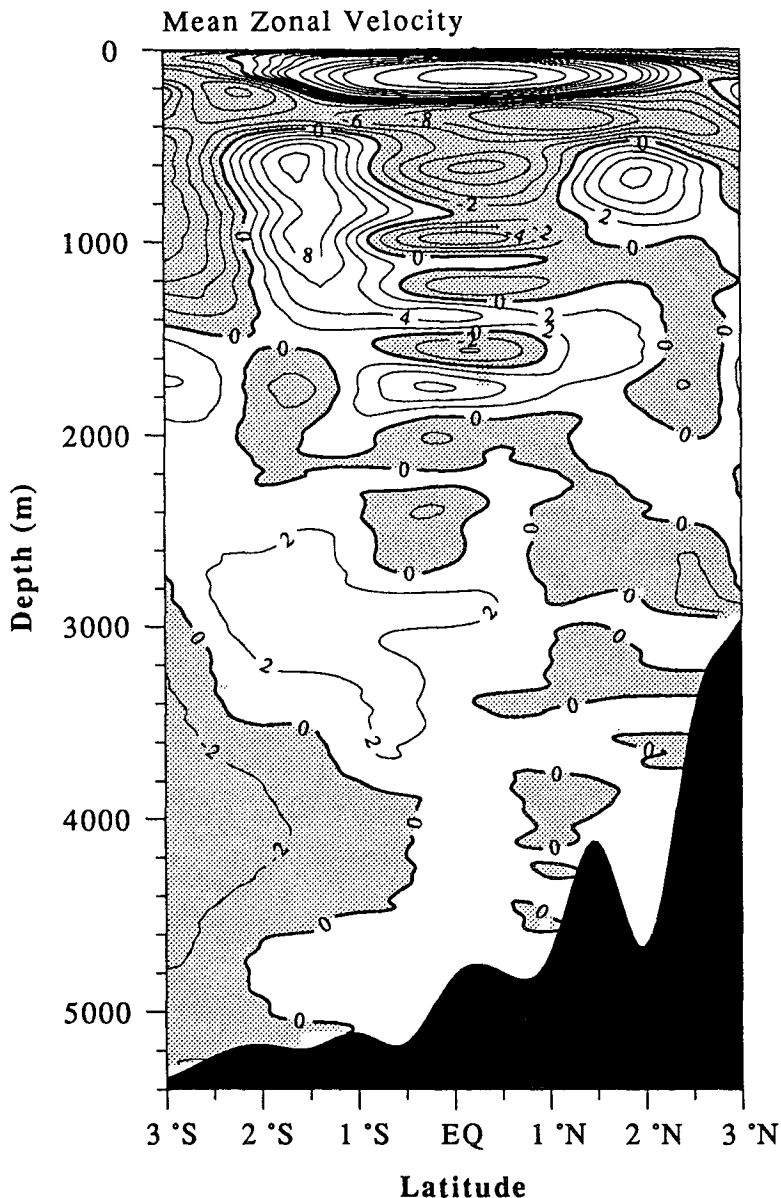
Mean Zonal Velocity

FIG. 4. Average zonal velocity from 41 Pegasus transects of the equator. Contour intervals are 2 cm s^{-1}. Major current features include the 50-cm s^{-1} Equatorial Undercurrent between 50–250 m, the 10 cm s^{-1} South and North Intermediate Countercurrents at 2°N and S between 400 and 1400 m, and the ±5-cm s^{-1} deep equatorial jets between 500 and 2500 m. The deep equatorial jets have vertical wavelengths of ~330 m.

measures temperature poorly and salinity not at all. We limit our reliance on the temperature measurements by assuming the mean zonal currents to be in geostrophic balance. Arthur (1960) first demonstrated the applicability of geostrophy on the equator. Assuming a geostrophic balance on the equator has become fairly commonplace since Eriksen (1982) showed the geostrophic nature of the jets and used density profiles in the Atlantic to infer the presence of equatorial deep jets there. Lukas and Firing (1984) and Moum et al. (1987) have demonstrated the importance of temporally or spatially averaging the dynamic height field to filter out internal waves before calculating near-equatorial geostrophic velocity.

Given that mean zonal velocity is in geostrophic balance, buoyancy can be calculated by meridionally integrating the thermal wind balance [Eq. (2b)]:
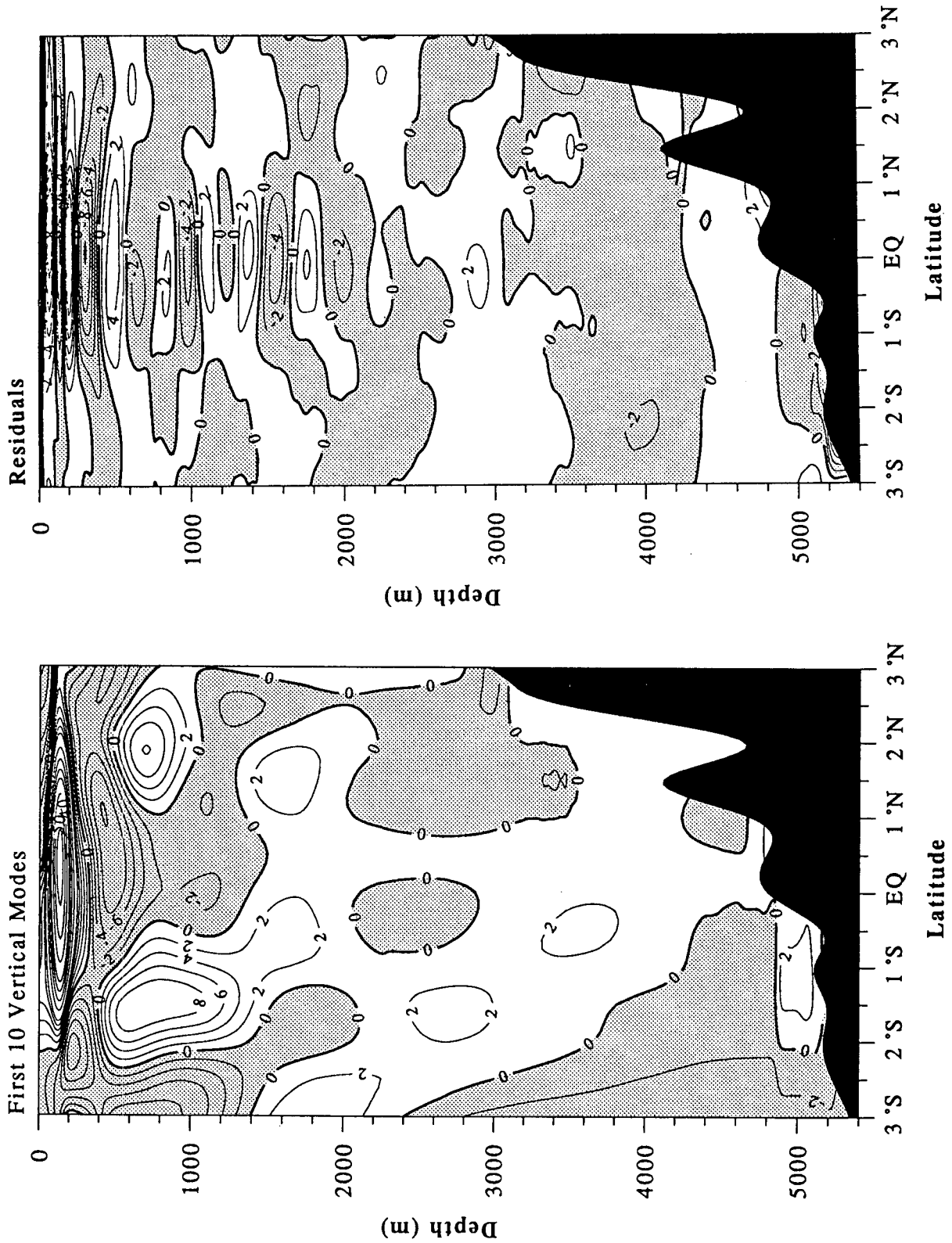
FIG. 5. Meridional structure of the (a) low-mode and (b) residual mean zonal currents. Note the continuation of the deep jets into the upper 300 m of the residual zonal velocity.
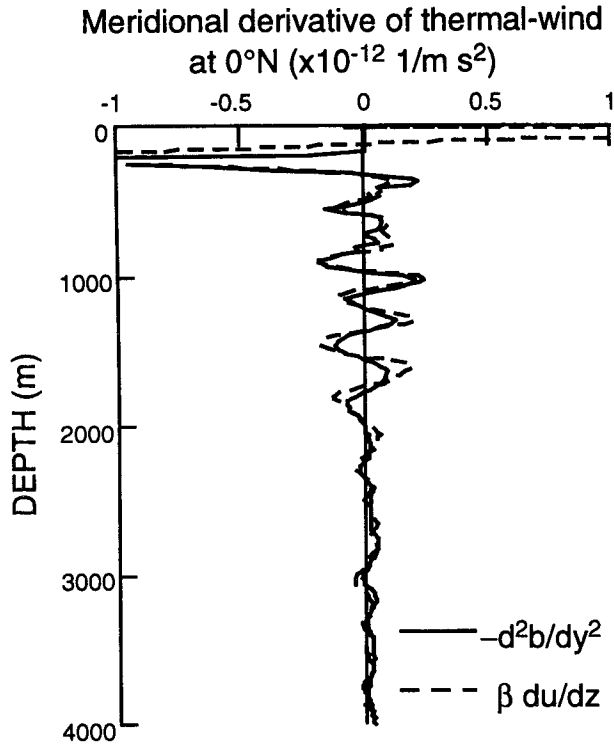
Meridional derivative of thermal-wind at 0°N (×10⁻¹² 1/m s²)

FIG. 6. Comparison of the meridional gradient of thermal-wind terms [Eq. (6)] at 0° as a test of geostrophy.

$$b_g(y) = b_T(y_0) - \int_{y_0=3°S}^{y} \beta y' \partial u / \partial z \, dy'. \quad (5)$$

The subscripts g and T indicate buoyancy calculated from temperature data or geostrophically, respectively. The low-mode and residual components of the velocity were integrated separately to yield corresponding components of the buoyancy. The integration proceeded from $y_0 = 3°S$; the 3°S buoyancy profile was calculated from Pegasus temperature and T-S information and separated into low-mode and residual components using a modal decomposition. It is recognized that the physical modes of buoyancy and velocity may not be the same, so the decomposition was applied only to separate the high- and low-wavenumber components of the initial buoyancy as a basis for integration. The sum of the calculated low-mode and residual buoyancies shows reasonable agreement with the buoyancy calculated from the density structure at 3°N calculated from Pegasus temperature data and T-S information (Fig. 7).

As a check of geostrophy, and on the quality of the time-mean horizontal temperature gradients, the terms of the meridionally differentiated thermal wind relation are compared,

$$\beta \partial u / \partial z = -\partial^2 b_T / \partial y^2 \quad \text{at} \quad y = 0. \quad (6)$$

Agreement between the terms is good (Fig. 6).

With the modal decomposition, the zonal velocity and buoyancy have two components (marked by subscripts),

$$u = u_l + u_r,$$

$$b_g = b_l + b_r,$$

so the potential vorticity may be broken up into low-mode and residual components,

$$q_l = \beta y N^2 - N^2 \frac{\partial u_l}{\partial y} + \beta y \frac{\partial b_l}{\partial z} - \frac{\partial u_l}{\partial y} \frac{\partial b_l}{\partial z} - \beta y \frac{\partial u_l^2}{\partial z}, \quad (7)$$

$$q_r = -N^2 \frac{\partial u_r}{\partial y} + \beta y \frac{\partial b_r}{\partial z} - \frac{\partial u_r}{\partial y} \frac{\partial b_l}{\partial z} - \frac{\partial u_l}{\partial y} \frac{\partial b_r}{\partial z} - \frac{\partial u_r}{\partial y} \frac{\partial b_r}{\partial z}$$

$$- 2\beta y \frac{\partial u_l}{\partial z} \frac{\partial u_r}{\partial z} - \beta y \frac{\partial u_r^2}{\partial z}. \quad (8)$$

The mixed terms of low-mode and residual zonal velocity and buoyancy have been included in the residual potential vorticity because they contain the smaller vertical scales of the residuals. Terms will be studied individually in the analysis, allowing the mixed terms to be identified separately.

For both low-mode and residual vorticity, the planetary vorticity is the only significant contributor to the potential vorticity in many locations. Relative vorticity, $u_y N^2$, and vortex stretching, $\beta y b_z$, also contribute significantly in some regions in each decomposition,
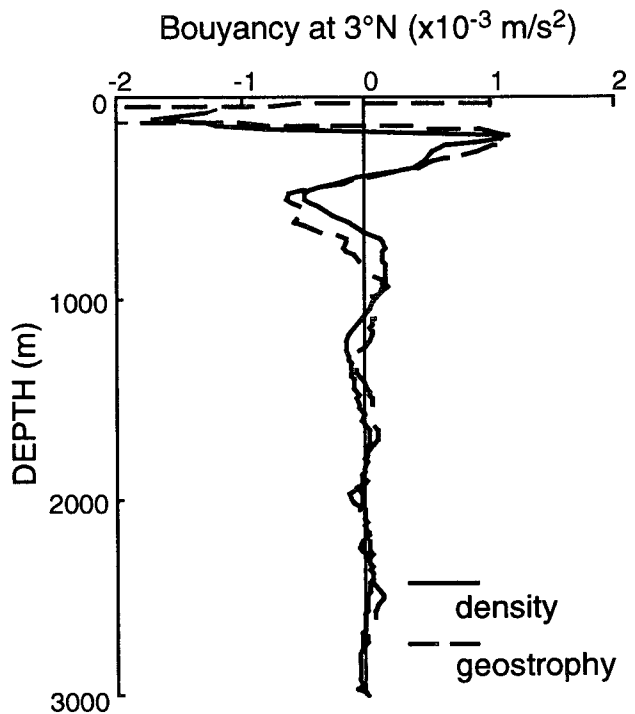
Bouyancy at 3°N (×10⁻³ m/s²)

FIG. 7. Buoyancy at 3°N from meridional integration of thermal-wind (dashed) and directly measured density structure (solid).
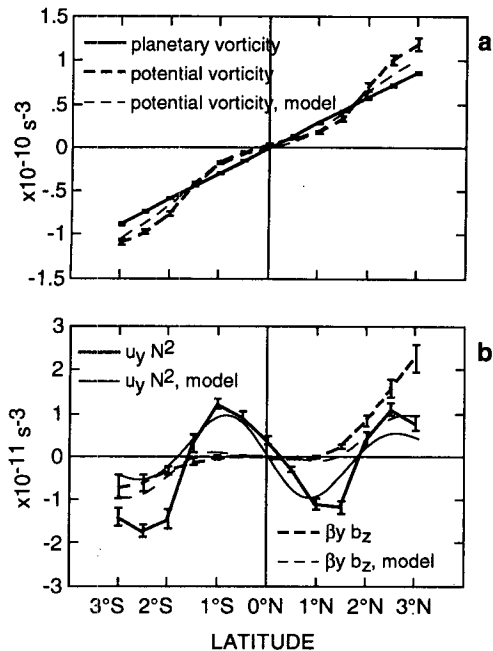
FIG. 8. (a) Planetary vorticity (solid line) and potential vorticity (dashed line) of modes 1–10 at 640 m. The light lines in both figures represent the theoretical results for the meridional-mode-3 Rossby wave discussed in section 4. (b) The wide plateau in potential vorticity about the equator is caused by the sum of relative vorticity (u_yN^2, solid line) and vortex stretching ($\beta y b_z$, dashed line).

reaching approximately 20% of βyN^2, the planetary vorticity. The nonlinear vorticity/stretching, u_yb_z, and the twisting term, βyu_z^2, are never statistically significant. The standard error of each term was calculated using the bootstrap method with 50 samples (Efron and Gong 1983).

3. Observations

a. Modes 1–10

In the absence of motion, the potential vorticity would be proportional to the planetary vorticity, which increases linearly with latitude. Instead the low-mode potential vorticity at 640-m depth plateaus near the equator, then increases steeply with latitude 1°–2° from the equator (Fig. 8a). The reduced slope near the equator is an effect of relative vorticity (Fig. 8b). Relative vorticity reaches extrema about 1° from the equator; farther from the equator it tends to steepen the slope of potential vorticity. Vortex stretching becomes significant at about 1.5°N and S, where it also increases the slope of potential vorticity.

This pattern of relative vorticity and vortex stretching creates a plateau in the potential vorticity that extends downward for several hundred meters. Below 1300 m, both relative vorticity and vortex stretching are noisy. Relative vorticity shows evidence of smaller scale meridional perturbations, but the difference be-

tween the planetary and potential vorticities is not statistically significant at these depths.

In summary, the potential vorticity calculated from the low-mode components of zonal velocity shows a coherent pattern from 400- to 1000-m depth. Relative vorticity is strongly antisymmetric about the equator throughout these depths, while vortex stretching fluctuates irregularly.

b. Residuals

As shown in Eq. (8), the potential vorticity of the residual consists of many components, including mixed terms between low-mode terms and high-wavenumber residuals. Of the purely residual terms, the only two that are statistically significant are relative vorticity, u_yN^2, and vortex stretching, βyb_z. A plot of these two components through a westward jet at 620-m is shown in Fig. 9a. At 0° the relative vorticity is nearly zero, it has a local maximum (minimum) between 1.0° and 1.5°S (1.5° and 2.0°N), then returns toward zero at 3°N and S. The vortex stretching follows a similar pattern but with maxima slightly larger in magnitude and farther poleward, between 1.5° and 2.0°S (1.5° and 2.0°N). This pattern in relative vorticity and vortex stretching is repeated in other westward jets. An eastward jet at 1120 m (Fig. 9b) most clearly illustrates the similarity between relative vorticity and vortex stretching; again vortex stretching is larger and has ex-
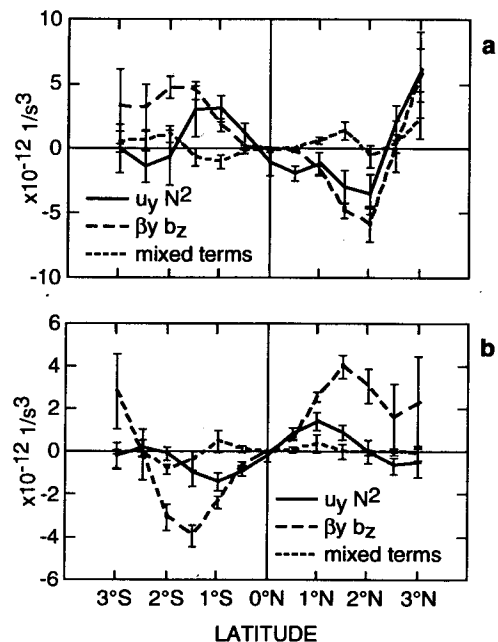

FIG. 9. Relative vorticity (u_yN^2, solid line) and vortex stretching (u_yb_z, dashed line) for the residuals (a) at 620 m, the depth of a westward jet and (b) at 1120 m, the depth of an eastward jet. Vortex stretching is larger in magnitude and has extrema farther off the equator than relative vorticity.

trema farther off the equator compared to the relative vorticity. The components of potential vorticity become increasingly noisy with depth; below 2500 m they are no longer statistically significant.

The only statistically significant nonlinear term in the residual calculation is the nonlinear vorticity/stretching, $\partial u_l / \partial y \partial b_r / \partial z$. This term is significant only in the upper 1000 m where the meridional gradient of low-mode zonal velocity is large. In this region, the mixed term is roughly one-third the magnitude and in opposition to the residual relative vorticity (Fig. 9a). It can be thought of as creating an effective beta felt by motions of shorter vertical scale, $\beta_{eff} = \beta + (u_l)_{yy}$. However, $(u_l)_y$ is larger than βy only between 30'N and S, indicating that the low-mode zonal velocity structure alters the effective beta only within 30' of the equator.

4. Models

Equatorial modelers have described the deep jets as Kelvin and long Rossby waves (e.g., Wunsch 1977; Ponte 1989). To further explore this hypothesis, we model both types of waves using parameters constrained by the data, then compare the results with the observed fields. The vertical wavelength in the models is 330 m, with maximum zonal velocity of 4 cm s^{-1}. In the very low-frequency regime (periods greater than one year), neither the period nor the zonal wavelength influence the meridional structure, which may be nondimensionalized as $\eta = (\beta k_z / N)^{1/2} y$. Likewise, components of potential vorticity are independent of both period and zonal wavelength for very low-frequency long waves.

a. Kelvin waves

McCreary and Lukas (1986) modeled the deep jets as Kelvin waves generated by a stationary wind patch on a westward barotropic current. Ponte (1989) modeled them as Kelvin waves forced at depth at the western boundary.

Kelvin waves do not perturb potential vorticity; vortex stretching balances relative vorticity, and twisting balances nonlinear vorticity/stretching exactly (Fig. 10a). This is not consistent with the observed potential vorticity signal (Fig. 9). Furthermore, the dominant terms in the observations, vortex stretching and relative vorticity, are of the same sign within 2° of the equator.

b. Rossby waves

1) FIRST-MERIDIONAL MODE (HIGH-WAVENUMBER JETS)

A first-meridional-mode Rossby wave has relative vorticity and vortex stretching of the same sign near the equator, with the vortex stretching relatively small very near the equator and reaching extrema poleward
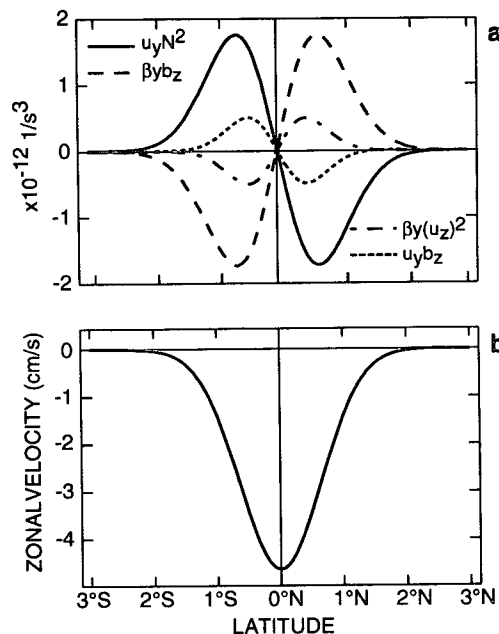

FIG. 10. The potential vorticity of Kelvin wave is entirely planetary vorticity, as the other components (a) sum to zero. (b) The zonal velocity of a Kelvin wave (cm s^{-1}).

of the relative vorticity extrema (Fig. 11), similar to the observed structure (Fig. 9). Meridional velocities of very low-frequency long waves are too small to be observed in the data. The resemblance of the modeled and observed zonal velocity structures suggests that the deep jets are Rossby waves, as does the similarity of the model potential vorticity and the potential vorticity of the residuals.

One contradiction between the model and the observations is the location of the zero crossings in zonal velocity. The broad meridional scale is consistent with previous observations of the deep jets (O'Neill and Luyten 1984; Ponte and Luyten 1989). The zero crossings of the jets are at roughly 1.5°N and S, while a Rossby wave of appropriate vertical wavelength (~330 m) has zero crossings at about 1°N and S. The meridional scale depends on the beta effect, the vertical wavelength, and the buoyancy frequency, all of which are well constrained by the data. The low-mode background flow could produce an "effective beta" through its potential vorticity. However, as discussed earlier, the observed low-mode potential vorticity cannot explain the meridional scales observed. Other possible explanations for the broad meridional scale will be discussed in section 5.

2) LOW-WAVENUMBER VELOCITY

As an aside to the analysis of the deep jets, the symmetric structure of the low-mode potential vorticity in the upper 1000 m (Fig. 8) also resembles a Rossby
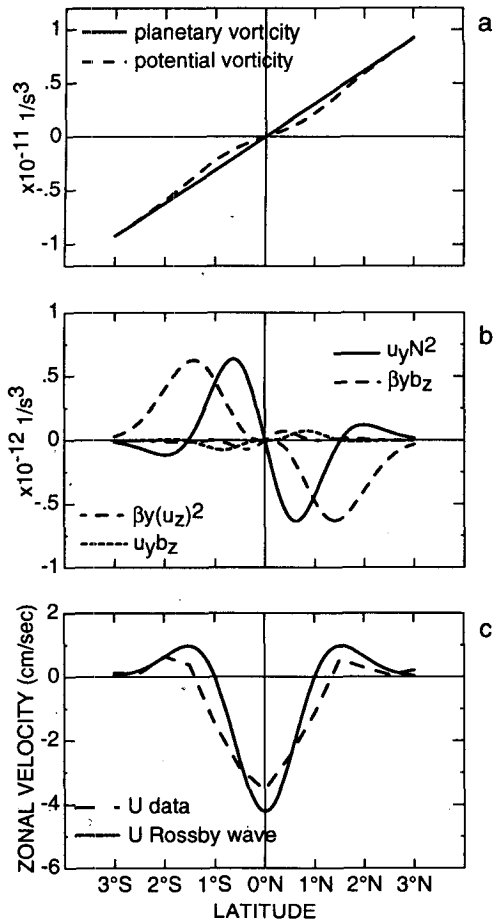
FIG. 11. First-meridional-mode long Rossby wave (a) potential vorticity signal, (b) components of potential vorticity, and (c) velocity structure. The dashed line in (c) represents the observed zonal velocity of a mean deep jet. Like the observed jets, the Rossby wave has off-equatorial current reversals, although in the model the reversals occur 30' equatorward of the observations.

observations is that the observed zero crossings in zonal velocity are 30' poleward of those predicted by linear theory. One explanation of the broader scale of the observations is a description of the jets as the sum of several meridional modes. A model jet with zero crossings at 1.5°N and S may be created using odd Rossby wave modes. The meridional scale of the potential vorticity broadens as well.

A description of the jets as a sum of Rossby waves is not entirely consistent with the observations. The individual wave components will propagate at different zonal group velocities, due to differing zonal wavelengths. Therefore, the strength of the jets should vary, and some jets disappear as different components come in and out of phase. There is some variation in strength of the jets over time, but in general, the jets persist over the 16 months of observations. It is conceivable that all of the wave modes were in phase with each other during the observational period, but this seems unlikely.

Another explanation for the broad meridional trapping scale is that the observed meridional scale may not be well resolved in the presence of higher-frequency meridional motions. Rossby gravity waves of 30- to 90-day period could advect the jets' maxima and therefore broaden the observed mean width of the jets by up to 30' (Fig. 12). This explanation has the advantage of simplicity.

The forcing mechanism by which either a first-meridional-mode Rossby wave or sums of meridional modes could be established is not clear. Surface generation seems unlikely due to the effects of the strong shear of the equatorial undercurrent (Proehl 1990), although generation by fluctuations in thermocline depth is possible. Forcing on the western boundary is not feasible because although Kelvin waves reflecting off an eastern boundary do produce Rossby waves, the magnitude of the incident Kelvin wave would overwhelm any observations of reflected Rossby waves (Clarke 1983). Another possible forcing area is the

wave. The similarity between the potential vorticity structure of the data (heavy lines) and that of a third-meridional-mode Rossby wave (light lines) is striking. In both modeled wave and data, vortex stretching becomes significant starting at the first nonequatorial zero crossing of relative vorticity where both terms take the same sign. The Rossby wave resemblance in the mean is not observed throughout the time series, though, due to differences in temporal evolution of the low-mode equatorial current (the EIC) and the extra-equatorial currents (the SICC, the NICC, and the SEIC). The current on the equator from 500–1500 m shifted from westward at the beginning of the time series to eastward at the end (Fig. 3), with no corresponding reversal in the extra-equatorial currents.

5. Discussion

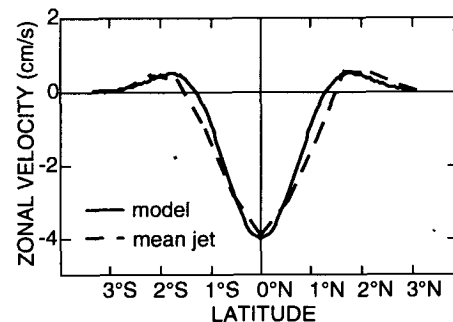The largest discrepancy between a model of the jets as a first-meridional-mode long Rossby wave and the

FIG. 12. A comparison between the observed zonal velocity signal of a mean deep jet and a model of the effect of meridional advection on the meridional structure of a long Rossby wave. The model is a first-meridional-mode long Rossby wave smoothed by a Gaussian of 30' half-width.
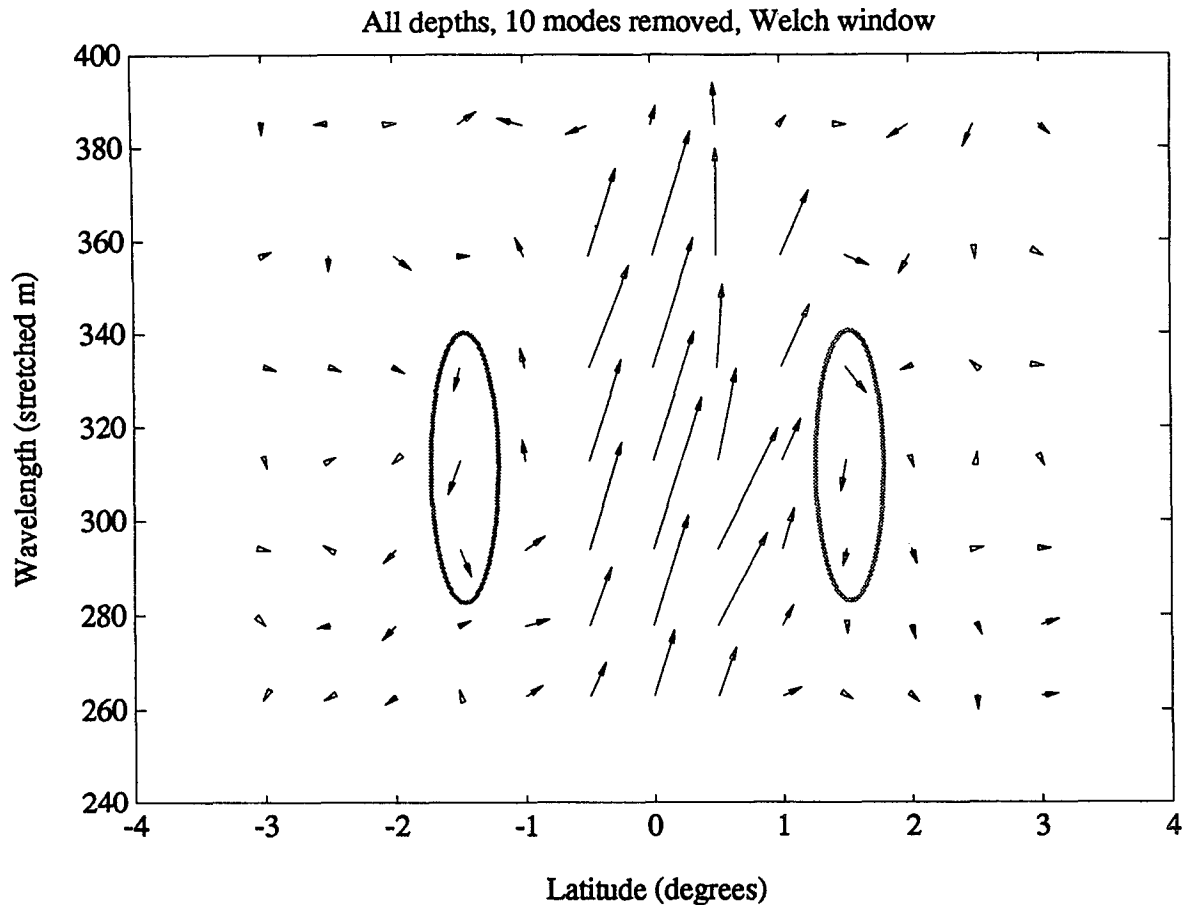
All depths, 10 modes removed, Welch window

FIG. 13. The amplitude and phase of zonal velocity vertical wavenumber components spanning the deep jet range. For each wavenumber, phases have been rotated such that the equatorial vector points 18° right of vertical. The first 10 modes have been removed, then the residual WKB stretched, scaled, windowed, and Fourier transformed. The grey ellipses emphasize the wavenumbers for which the phase at 1.5°N and S is reversed with respect to the equator.

eastern boundary, but there are too few observations of the circulation in the eastern equatorial Pacific to indicate any potential genesis mechanisms for the deep jets (Harvey and Patzert 1976; Lonsdale 1977).

All of these forcing mechanisms assume linear wave dynamics and require the sustenance of the jets over several wave periods. If the jets are periodic in time, their period must be at least several years to explain the lack of vertical motion in the observations. Therefore, it would take a decade to propagate a wave group into the ocean interior from either the surface or the eastern boundary. This is problematic in the presence of even small dissipation rates [$\epsilon \sim 10^{-9}$ W kg^{-1} in the deep equatorial ocean (Peters et al. 1988)], which would erode the deep jets on time scales of 1 to 6 years. Generation of the jets within the interior would avoid the long time scales involved in vertical propagation. Possible internal energy sources for the deep jets include internal instabilities and wave–wave interactions.

To illustrate how important the dissipative time scale is to the vertical propagation of the deep jets, a simple

model is developed. A period of 10 years is chosen from the phase propagation observed by Ponte and Luyten (1989); assuming the deep jets are first-meridional-mode long Rossby waves, the zonal wavelength will be $k_x \sim 10^7$ m (almost the width of the equatorial Pacific Ocean). If the deep jets were forced at the thermocline, several reflections from both eastern and western boundaries would be necessary to establish the observed vertical extent of the jets. The travel time of a long Rossby wave westward across the Pacific is approximately 12 years, while a Kelvin wave reflected from the eastern boundary would take 3 to 4 years to return across the basin. Ignoring energy loss in the reflection process, establishing the deep jets over the observed 1500-m depth range would take approximately 75 years. Deep forcing on the eastern boundary would require a similar time frame unless the forcing region was vertically extensive. Clearly neither model is feasible in the presence of any dissipative effects.

Very large values of ϵ have been observed in the high shear regions between the jets (Gregg et al. 1992). The

observed dissipation rates are sufficient to completely erode the jets in less than a month. Clearly this is not the case; perhaps the dissipation of higher-frequency motions is feeding momentum into the jets through critical-layer processes, thereby sustaining them.

6. Conclusions

The equatorial deep jets perturb potential vorticity, inconsistent with the hypothesis that the jets are Kelvin waves. The meridional structure of both potential vorticity and zonal velocity resembles that of a first-meridional-mode long Rossby wave. The main discrepancy between the observations and this model is the meridional scale, but the broad scale of the observed jets may be explained by meridional advection of the jets by higher-frequency meridional motions.

In retrospect, one need not have used potential vorticity to test the Rossby and Kelvin wave models. The difference between Rossby waves and a Kelvin wave lies solely in the meridional structure of zonal velocity; first-meridional-mode Rossby waves have a phase reversal off the equator, whereas the velocity structure of a Kelvin wave decays exponentially. The off-equatorial phase reversal in the deep jets can be seen both in the zonal velocity structure of the jets and in the phase relation of the wavelength bands associated with the deep jets. There is a distinct tendency toward a phase reversal at 1.5°N and S compared to 0° at the vertical wavelengths containing the deep jets (Fig. 13). This precludes the possibility of the jets being Kelvin waves but allows that they might be Rossby waves.

With little information about the zonal and temporal evolution of the deep jets it would be premature to definitively cast them as linear long waves. The observations are not inconsistent with a model of the jets as linear long Rossby waves, but they are insufficient to fully test such a model.

REFERENCES

Arthur, R. S., 1960: A review of the calculation of ocean currents at the equator. *Deep-Sea Res.,* **6,** 287–297.

Clarke, A. J., 1983: The reflection of equatorial waves from oceanic boundaries. *J. Phys. Oceanogr.,* **13,** 1193–1207.

Efron, B., and G. Gong, 1983: A leisurely look at the bootstrap, the jackknife and cross-validation. *Amer. Stat.,* **37,** 36–48.

Eriksen, C. C., 1981: Deep currents and their interpretation as equatorial waves in the western Pacific Ocean. *J. Phys. Oceanogr.,* **11,** 48–70.

——, 1982: Geostrophic equatorial deep jets. *J. Mar. Res.,* **40,** 143–157.

——, 1985: Moored observations of deep low-frequency motions in the central Pacific Ocean: Vertical structure and interpretation as equatorial waves. *J. Phys. Oceanogr.,* **15,** 1085–1113.

——, and J. G. Richman, 1988: An estimate of equatorial wave energy flux at 9- to 90-day periods in the central Pacific. *J. Geophys. Res.,* **93,** 15 455–15 466.

Firing, E., 1987: Deep zonal currents in the central equatorial Pacific. *J. Mar. Res.,* **45,** 791–812.

——, 1988: Shallow equatorial jets. *J. Geophys. Res.,* **93,** 9213–9222.

——, 1989: Mean zonal currents near the equator below 1500 m. *J. Geophys. Res.,* **94,** 2023–2028.

Gregg, M. C., T. B. Sanford, and D. P. Winkel, 1992: From the San Diego trough to equatorial deep jets. *Eos, Trans., Am. Geophys. Union,* **73**(Suppl.), 320 [abstract].

Harvey, R. R., and W. C. Patzert, 1976: Deep current measurements suggest long waves in the eastern equatorial Pacific. *Science,* **193,** 883–885.

Hayes, S. P., and H. B. Milburn, 1980: On the vertical structure of velocity in the eastern equatorial Pacific. *J. Phys. Oceanogr.,* **10,** 633–635.

Lonsdale, P., 1977: Inflow of bottom water to the Panama Basin. *Deep-Sea Res.,* **24,** 1065–1101.

Leetmaa, A., and P. F. Spain, 1981: Results from a velocity transect along the equator from 125° to 159°W. *J. Phys. Oceanogr.,* **11,** 1030–1033.

Lukas, R., and E. Firing, 1984: The geostrophic balance of the Pacific Equatorial Undercurrent. *Deep-Sea Res.,* **31,** 61–66.

Luyten, J. R., and J. C. Swallow, 1976: Equatorial undercurrents. *Deep-Sea Res.,* **23,** 499–524.

McCreary, J. P., 1984: Equatorial beams. *J. Mar. Res.,* **42,** 395–450.

——, and R. Lukas, 1986: The response of the equatorial ocean to a moving wind field. *J. Geophys. Res.,* **91,** 11 691–11 705.

McPhaden, M. J., J. A. Proehl, and L. M. Rothstein, 1986: The interaction of equatorial Kelvin waves with realistically sheared zonal currents. *J. Phys. Oceanogr.,* **16,** 1499–1515.

Millard, R. C., W. B. Owens, and N. P. Fofonoff, 1990: On the calculation of the Brunt–Väisälä frequency. *Deep-Sea Res.,* **37,** 167–181.

Moum, J. N., T. K. Chereskin, M. M. Park, and L. A. Regier, 1987: Monitoring geostrophic currents at the equator. *Deep-Sea Res.,* **34,** 1149–1161.

O'Neill, K., and J. R. Luyten, 1984: Equatorial velocity profiles. Part II: Zonal component. *J. Phys. Oceanogr.,* **14,** 1842–1852.

Peters, H., M. C. Gregg, and J. M. Toole, 1988: On the parameterization of equatorial turbulence. *J. Geophys. Res.,* **93,** 1199–1218.

Ponte, R. M., 1989: A simple model for deep equatorial zonal currents forced at lateral boundaries. *J. Phys. Oceanogr.,* **19,** 1881–1981.

——, and J. R. Luyten, 1989: Analysis and interpretation of deep equatorial currents in the central Pacific. *J. Phys. Oceanogr.,* **19,** 1025–1038.

——, ——, and P. L. Richardson, 1990: Equatorial deep jets in the Atlantic Ocean. *Deep-Sea Res.,* **37,** 711–713.

Proehl, J. A., 1990: Equatorial wave–mean flow interaction: The long Rossby waves. *J. Phys. Oceanogr.,* **20,** 274–294.

Wunsch, C., 1977: Response of an equatorial ocean to a periodic monsoon. *J. Phys. Oceanogr.,* **7,** 497–511.